Observation of Massive Overcompensation in the Complexation of Sodium Poly(styrenesulfonate) with Cationic Polymer Micelles

M. Ruela Talingting, Ulrike Voigt, Petr Munk, and S. E. Webber*

Department of Chemistry and Biochemistry and Center for Polymer Research, The University of Texas at Austin, Austin, Texas 78712

Received August 3, 2000; Revised Manuscript Received October 31, 2000

ABSTRACT: Complex particles have been formed by the electrostatic association of protonated polystyrene-*b*-poly(2-vinylpyridine) (PS-*b*-PVPH$^+$) micelles with sodium poly(styrenesulfonate) (PSS$^-$Na$^+$), all at pH 1. Light scattering demonstrates that there is a large mass excess of PSS$^-$ associated with each PS-*b*-PVPH$^+$ micelle (the molecular weight increases by factors of 5−6), even in the limit that the weight ratio of the micelle to PSS$^-$Na$^+$ is very low, thereby avoiding bridged structures. This system is an example of charge and mass overcompensation, but to a much greater extent than usual. Surprisingly the effect of the molecular weight of the PSS$^-$Na$^+$ is minor. We believe that it is the flexible polymer micelle corona that permits such a large degree of mass and charge overcompensation because the linear PSS$^-$Na$^+$ can penetrate the micelle corona and adopt a convoluted local conformation with many loops or points of grafting attachment. While these particles are stable with respect to storage, they do not seem to be stable to centrifugation or filtration. The former instability is ascribed to the concentrating of the complex micelle as centrifugation proceeds while the latter suggests these particles are not stable with respect to shear.

Introduction

The interaction of linear polyelectrolytes with oppositely charged objects, including other polyelectrolytes, has been studied in a variety of different contexts. Some of this effort has been motivated by practical applications such as stabilization of colloids or control of flocculation.[1] In some cases such as controlled deposition of polyelectrolytes on surfaces,[2] purification of proteins,[3] or development of drug delivery systems,[4] technological applications seem likely. The outcome of these reactions depends on the overall charge balance between the two species and the molecular weight and charge density of the polyelectrolyte. If the interacting pairs achieve charge balance, there is a strong tendency for flocculation and precipitation to occur. Even if charge balance is not achieved, aggregation can occur by the formation of bridging structures.[5]

The present paper deals with the complexation of an anionic polyelectrolyte (sodium poly(styrenesulfonate), PSS) with a polymer micelle composed of polystyrene-*b*-poly(2-vinylpyridine) in pH 1 aqueous solution, which is sufficiently acid to protonate the pyridine groups that make up the micelle corona (denoted PS-*b*-PVPH$^+$ hereafter).[6] The PS-*b*-PVPH$^+$ micelle cannot remain in solution if the pH is greater than 5 because the pyridine groups deprotonate. In contrast, PSS is a strong electrolyte and is not appreciably protonated at pH 1. The interaction of a polyelectrolyte with an oppositely charged polymer micelle is analogous to the interaction of a polyelectrolyte with a latex or colloid particle, with one important difference: the charged corona of a polymer micelle is flexible and diffuse, permitting intercalation of the polyelectrolyte as the corona−polyelectrolyte complex is formed (Scheme 1). For a latex or colloid particle the charge is confined to a rigid surface, which suggests that a smaller relative mass of polyelectrolyte can be accommodated. We find that polymer micelle−polyelectrolyte complexes are formed in which the mass of adsorbed PSS is substantially larger than that of the polymer micelle. In the present study we also examine the effect of the molecular weight of the PSS polyelectrolyte over the range 5K to 801K. As one would expect, a high molecular weight PSS encourages the formation of aggregates because a single polymer can easily form bridging structures. In the limit of an infinitely low mass ratio of the polymer micelle to PSS, we believe we form monomeric complexes (i.e., no bridging structures). We find that the molecular weight of the monomeric complex increases systematically, but relatively weakly, with the molecular weight of the PSS.

Experimental Section

PS-*b*-PVPH$^+$ "Acid Micelles". We have previously reported the properties of the "acid micelles".[6] Our PS-*b*-PVP polymer micelle is composed of diblock polymers with degrees of polymerization for the polystyrene and poly(2-vinylpyridine) blocks of 377 and 580, respectively (molecular weight of diblock polymer ca. 10^5 g/mol). The final polymer micelle has a molecular weight of 13.4×10^6 g/mol, so the aggregation number of the polymer micelle is 134. The total number of pyridine groups is therefore $134 \times 580 \approx 7.7 \times 10^4$, which also represents the maximum charge of the polymer micelle if all the pyridine groups are protonated. Obviously, pyridine groups near the core−corona interface are less likely to carry charge because of the high local charge density that would result. The micelle hydrodynamic radius and radius of gyration are 49 and 33.8 nm, respectively. Because this micelle is stable only for pH < 5, we refer to it as an "acid micelle" (AM) herein. Unless stated otherwise, all experiments are at pH 1, which corresponds to an ionic strength of 100 mM. A small additional ionic strength is contributed by the counterions of the PVPH$^+$ and PSS (ca. 1 mM).

Sodium Poly(styrenesulfonate) (PSS). The sodium poly(styrenesulfonate) samples were obtained as a molecular weight standard kit from Scientific Polymer Products, Inc. The weight- and number-average molecular weights of the samples was stated to be as follows by the supplier: (1) 4950/4920, (2) 16 600/14 700, (3) 57 500/52 100, (4) 127 000/103 200, and (5) 801 100/691 300. According to elemental analysis, these polymers are approximately 94% sulfonated (private communication from the supplier).

10.1021/ma001366z CCC: $19.00
Published on Web 12/02/2000

Scheme 1

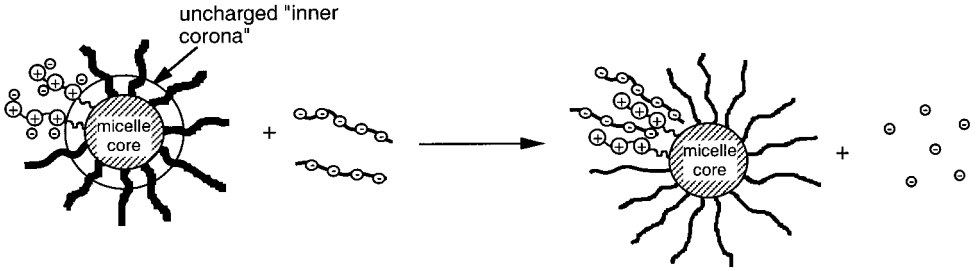

UV Absorption Protocol To Determine Acid Micelle Concentration. In the process of preparing acid micelles or the acid micelle−PSS complex, it is possible to experience loss of material by loss to dialysis tubing or filtration. Consequently, it is necessary to have a method of concentration analysis that is suitable for taking small aliquots from fairly dilute solutions. The extinction coefficient of the pyridine moiety is significantly larger than the phenyl group such that it is possible to determine the concentration of PS-*b*-PVPH$^+$ in the presence of PSS. The analysis procedure for the AM alone involved addition of aliquots of the micelle solution to 95:5 vol % ethanol:0.1 M NH_4OH(aq). This solvent mixture completely dissolves the micelles, and the presence of the NH_4-OH ensures the deprotonation of the pyridinium. Because the extinction coefficient is different for protonated or deprotonated pyridinium, it is essential to work with either excess base or acid in this step. A calibration curve was obtained using known concentrations of PS-*b*-PVP copolymers dissolved in THF injected into in the same solvent mixture. The absorption coefficient was found to be 19 754 au mL/(g cm) at 262 nm.

In the process of determining the concentration of PS-*b*-PVPH$^+$ in the presence of PSS, aliquots of the "onion" micelle solutions were added into the ammoniacal ethanol, and the absorbance was measured at 262 nm. However, the absorbance of PS-*b*-PVP increases with time even with stirring and shaking for about 30 min. The absorption spectra showed evidence of light scattering when a larger amount of micelle solution was used, manifested as a consistent increase in the baseline. We postulated that the excess PSS polyelectrolyte was not completely dissolved in the ammoniacal ethanol solvent, but it was possible to increase the solubility of the PSS by increasing the water content of the mixed solvent. By trial and error the following composition was obtained: 3.75:3.75:92.5 vol % water:0.1 M NH_4OH(aq):ethanol. When this was done, the light scattering of the resulting solution disappeared, and the absorbance reached a constant value within significantly less time (less than 5 min). However, to avoid these effects completely, the total volume of the aliquots added was less than 300 μL of approximately 1×10^{-5} g/mL polymer micelle solution added to 2.5 mL of solvent. The extinction coefficient at 262 nm was found to be 19 402 au mL/(g cm) in this solvent mixture.

Static Light Scattering. The Wyatt Technology Dawn B multiangle light scattering instrument was used in the static light scattering experiments (Wyatt Technology Corp.). The refractive index increments, dn/dc, were estimated from standard values for PVP and PS latexes in water.[6,7] The dn/dc of the PSS in acid water was determined to be 0.147 mL/g. In most experiments described herein 50 μL aliquots of the complex micelle solution were added to 10.0 mL of 0.1 M HCl (HPLC grade HCl diluted in ultrapure water was used). The maximum added volume was typically 250 or 300 μL (i.e., the original solution was diluted by a factor from 40 to 200). The intensity of scattered light was measured as a function of scattering angle and concentration to create Zimm plots.[8] Standard analysis of these plots using software provided by Wyatt yields information on the molecular weight, radius of gyration, and second virial coefficient of the micelles. The apparent MW ($(MW)_{app}$) was obtained using the dn/dc value for the pure AM, and the true molecular weight of the complex particle is determined for the "onion" morphology as discussed later (see eqs 1−3). The radius of gyration we report is based on the initial slope of a quadratic fit to the $\sin^2(\theta/2)$ dependence because there is some curvature at higher θ, which we assume is because of the relatively large size of the particles. The second virial coefficient is essentially zero within experimental error (magnitude ca. 1×10^{-5} mol mL/g^2 and fluctuating in sign), and we do not report the values. This is undoubtedly because our micelle concentration was so low (as low as ca. 5×10^{-5} mg/mL) and the relatively high ionic strength (ca. 100 mM). The concentration of the solutions could be determined after the light scattering was complete, using the UV absorption method discussed above. This was essential for filtered solutions because of loss of material to the filter.

Refractive Index Increment for PSS in pH 1 HCl. The refractive index increment (dn/dc) of PSS at 632.8 nm was measured using a Brice-Phoenix differential refractometer model BP-2000-V from Phoenix Precision Instruments Co. The procedure required determining the instrument calibration factor using NaCl solutions of known dn/dc.[9] The dn/dc value was then determined by measuring the change of the refractive index of the solvent when the sample is added.[10] The dn/dc was measured for PSS with MW = 801 000. The sample was dissolved in 0.1 M HCl and stirred overnight. The average dn/dc for the PSS solution in 0.1 M HCl was calculated to be 0.147 ± 0.002.

Zetaplus and QELS Measurements. A BIC Zetaplus potential analyzer with BI-9000 AT digital correlator (Brookhaven Instruments Corp.) was used for the determination the distribution of hydrodynamic diameters and ζ-potential. In this instrument the quasi-elastic light scattering (or dynamic light scattering) is measured at 90° scattering angle using a solid-state laser with wavelength 670 nm. Various data analysis schemes are available as part of the software package from Brookhaven, and we chose to present the results using the "log normal" distribution by weight.[11] We find this method provides a relatively stable characterization of the complex particles described herein, whereas the non-negatively constrained least-squares method (NNLS), which can yield the distribution of particle sizes in principle, did not provide data that varied systematically with the mass ratio of the AM to PSS (see later).

For determination of the electrophoretic mobility approximately 2 mL of solution was placed inside a plastic cuvette, the electrode cap was then placed inside the cuvette and bubbles are removed by gentle tapping. The micelle solutions as prepared have too high an ionic strength for this technique because the higher current may heat up the solution. Therefore, it was necessary to reduce the ionic strength below 0.05 M. The complex micelle solution was stepwise dialyzed against 0.05 M NaCl, 1×10^{-3} M NaCl, 1×10^{-5} M NaCl, and 1×10^{-7} M NaCl at pH 7 to achieve micelle solutions with these ionic strengths. As will discussed in the main text, it was not obvious to us that the micelles would survive this process.

SEM. SEM images were obtained using a Philips 515 scanning electron microscope, which was equipped with a Polaroid camera. For the size and nature of the micelles on surfaces, a higher accelerating voltage of electrons and bias (25 kV and 3, respectively) and smaller beam spot size of 20 nm were found to improve the image of the micelles. All SEM samples were sputter-coated with ca. 10 nm of Au−Pd on a Ladd benchtop sputter coater using a 60/40 Au/Pd target at 2.5 kV/20 mA for 45 s. Quartz surfaces were aminated by the

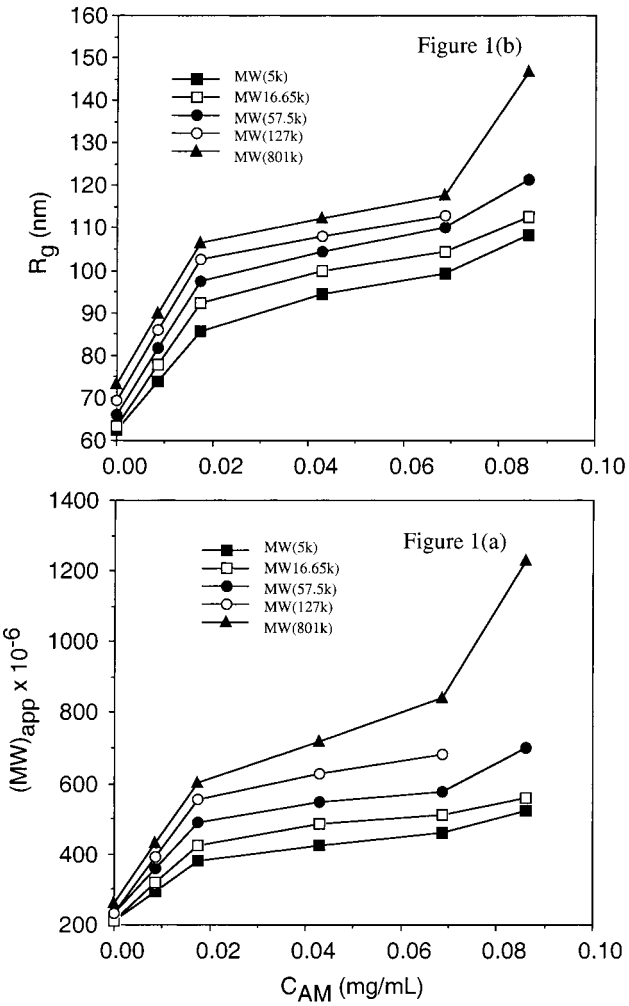

Figure 1. (a) $(MW)_{app}$ vs c_{AM} for different molecular weights of PSS. (b) $(R_g)_{app}$ vs c_{AM} for different molecular weights of PSS. The two lowest data points are extrapolated to $c_{AM} = 0$ to obtain $(MW)^0_{app}$ and R_g^0 (see text). The concentration of PSS is constant (0.227 mg/mL), and the pH is 1.

reaction with (3-aminopropyl)dimethylethoxysilane. Just before attachment of the complex micelle the surface is soaked in 0.1 N HCl for 5 min, and then the surface was placed in contact with the AM/PSS solution.[12]

Observations

Preparation of PSS and AM Complexes at pH 1. The order of mixing solutions of PSS and the acid micelle is critical to the nature of the final solution. Adding different aliquots of 2.75 mg/mL AM to 1 mL of 0.25 mg/mL of the PSS in pH 1 solution yields a strongly scattering solution up to the point that the AM/PSS mass ratio is approximately 0.5. Above this mass ratio a precipitate begins to form, even though charge neutralization is probably not achieved (see later discussion). We assume the precipitate formed under these conditions is a consequence of the bridging mechanism. Dilution of the mixture with pH 1 water (HCl) to a constant volume was then carried out (final concentration of PSS was 0.227 mg/mL). It is important to keep the tip of the micropipet under the level of the rapidly stirred PSS solution during the injection.

If a solution of PSS is injected into a solution of the acid micelle, a precipitate forms immediately. We assume this is because during the initial stages of the injection the ratio of PSS to acid micelle is low, which enhances the formation of bridging structures or neutral particles. The irreversibility of the precipitation suggests that bridging structures may be kinetically trapped, and therefore structures formed by simple mixing may not be the thermodynamic minimum.

Table 1. Static Light Scattering Data (Based on Quadratic Fit)

MW (PSS)	c_{AM} (mg/mL)[a]	$(MW)_{app}/10^6$ (g/mol)	R_g (nm)[b]	$(R_h)_{eff}$ (nm) (PD)[c]
5K	8.65×10^{-3}	295 ± 20	74.0	61.7 (0.200)
	1.73×10^{-2}	380 ± 30	85.7	67.5 (0.223)
	4.30×10^{-2}	426 ± 10	94.4	43.5 (0.128)
	6.87×10^{-2}	462 ± 8	99.2	58.3 (0.180)
	8.60×10^{-2}	523 ± 7	108.2	59.6 (0.192)
16.6K	8.65×10^{-3}	318 ± 40	77.8	55.3 (0.180)
	1.73×10^{-2}	426 ± 10	92.3	51.6 (0.141)
	4.30×10^{-2}	485 ± 10	99.8	56.9 (0.171)
	6.87×10^{-2}	511 ± 10	104.3	55.4 (0.192)
	8.60×10^{-2}	558 ± 8	112.6	59.8 (0.087)
57.5K	8.65×10^{-3}	360 ± 20	81.8	60.3 (0.214)
	1.73×10^{-2}	489 ± 20	97.5	59.5 (0.163)
	4.30×10^{-2}	549 ± 9	104.5	43.5 (0.128)
	6.87×10^{-2}	577 ± 8	110.2	NA
	8.60×10^{-2}	701 ± 10	121.2	63.1 (0.176)
127K	8.65×10^{-3}	393 ± 8	86.0	57.8 (0.189)
	1.73×10^{-2}	554 ± 20	102.5	65.3 (0.183)
	4.30×10^{-2}	626 ± 10	108.1	65.6 (0.184)
	6.87×10^{-2}	682 ± 20	112.8	67.8 (0.181)
	8.60×10^{-2}	NA	NA	68.3 (0.174)
801K	8.65×10^{-3}	433 ± 10	90.0	52.9 (0.306)
	1.73×10^{-2}	603 ± 20	106.6	68.3 (0.182)
	4.30×10^{-2}	720 ± 20	112.2	66.2 (0.153)
	6.87×10^{-2}	840 ± 20	117.6	68.1 (0.164)
	8.60×10^{-2}	1230 ± 20	146.6	81.7 (0.170)

[a] Concentration of PSS^-Na^+ 0.227 mg/mL for all solutions. [b] $R_g = \sqrt{(R_G)^2_{app}}$. [c] Obtained from the log-normal analysis of QELS.

The apparent molecular weight (MW_{app}) of the AM−PSS complex measured by SLS increases steadily with the AM concentration at constant PSS concentration (Figure 1a and Table 1). For a given AM/PSS mass ratio a higher PSS molecular weight yields a higher molecular weight complex. However, considering the range of molecular weight used (a factor of 160), this effect is not so large. Likewise, the apparent R_g increases with the AM/PSS mass ratio, with essentially equal slope for the range 0.02−0.07 g/mL of acid micelle (Figure 1b and Table 1). The exact values of these quantities depend on the analysis of the Zimm plot. Because of the size of these particles, we tend to favor the quadratic fit to the $\sin^2(\theta/2)$ ($c = 0$) extrapolated line, but the qualitative effects are the same no matter what kind of data analysis is carried out. As the concentration of the AM decreases, the values of $(MW)_{app}$ and R_g ($= \sqrt{(R_G)^2_{app}}$) for all molecular weights of PSS tend to converge. The most straightforward interpretation of these data is that a small fraction of multicentered bridged aggregates form as the AM/PSS ratio increases. We note that under the conditions of the SLS experiment any weakly bound aggregates are likely to dissociate because the stock solutions are diluted by a factor of at least 40 (see Experimental Section). Furthermore, the approximately linear concentration dependence of the SLS signal, which is part of the standard Zimm plot analysis, confirms that there is no dynamic dissociation equilibrium over the concentration range used. Hence, we conclude that the complex particles formed initially are stable at low concentration (but not necessarily against hydrodynamic flow or upon concentration, as will be discussed later).

The sensitivity of our QELS apparatus is much lower than the SLS instrument, such that QELS measurements were made on the solutions as prepared without further dilution. There are several ways to analyze QELS data using the software package supplied by Brookhaven Instruments. The NNLS algorithm provides a distribution of hydrodynamic diameters weighted by the scattering intensity. We primarily wanted to verify that there were no large particles present in solution, as would be the case if bridging occurs. We typically observed a multimodal distribution of hydrodynamic diameters, especially for the higher molecular weight PSS. We found the "log normal" method provides a more robust characterization of the particle size distribution, as discussed in the Experimental Section. The hydrodynamic radii ($(R_h)_{eff}$) and polydispersity from this latter mode of analysis are collected in Table 1. There is essentially no variation of these parameters with the molecular weight of the PSS at the lower concentrations of the acid micelle and no systematic variation with the AM/PSS mass ratio.

We wished to examine the effect of kinetics on the properties of the complex particle. Therefore, a sample was prepared using PSS(57.5K) with a final mass ratio of AM to PSS of 0.25. However, the AM stock solution was diluted by a factor of 4, therefore requiring 4 times more volume to be injected into the PSS solution. The apparent molecular weight and R_g of the complex particle were 346×10^6 and 93.2 nm, respectively, which are reasonably close to the expected values based on the data in Table 1. We note that these values are most similar to the smallest AM/PSS weight ratio for the PSS(57.5K) preparation, which suggests that so long as there is a large excess of PSS, a sufficiently low concentration of AM at the point of injection will yield "monomeric" AM/PSS complex particles (see next section).

The association between the PSS and the cationic micelle is favored because of the strong electrostatic attraction. The Debye length in pH 1 HCl is approximately 0.96 nm so there is no long-range electrostatic interaction between the AM and the PSS. It is interesting to consider the charge balance that exists in the PSS and AM solutions as initially prepared. The PSS concentration is constant, 0.227 mg/mL, equivalent to 1.17 mM in styrenesulfonate groups[13] The maximum charge on the acid micelle is related to the number of pyridine moieties, which constitute 0.62 of the micelle by mass. The acid micelle concentration ranges between 8.65×10^{-3} and 8.60×10^{-2} mg/mL, which corresponds to 0.0501−0.504 mM in pyridine groups. Therefore, even if all the pyridine groups are protonated, there is a significant excess of negative charge available from the styrenesulfonate groups. The point at which we typically observe precipitation (ca. 0.10−0.15 mg/mL of AM depending on the molecular weight of the PSS) corresponds to a charge neutralization of ca. 0.59−0.88 by this calculation. Since the pyridine groups are unlikely to be 100% charged, it is reasonable to associate the formation of a precipitate with charge neutralization of the complex particle in addition to the possible formation of bridging structures. For the lower concentrations of acid micelles it seems to us that the ca. 23 times excess of PSS should minimize the formation of bridging structures. It is also the case that as the association of the AM and PSS proceeds, the complex particle must pass through a point of zero net charge, at which point some aggregates could form, a process which should be minimized at low AM concentration. Therefore, we consider the results extrapolated to zero concentration of AM as the most reliable, and it is this limit we discuss in the following.

Table 2. SLS Data in the Limit $c_{AM} \rightarrow 0$ (Monomeric "Complex Micelle" (cm)) (Based on Quadratic Fit)

MW (PSS)/10^3	$(MW)^0_{app}$/ 10^6 g/mol	δ^0	$(MW)^0_{cm}$/ 10^6 g/mol	R_g^0	$(R_g^0)_{outer}$[a] (nm)
5	210	5.41	72.5	62.3	69.3
16.6	210	5.41	72.5	63.3	70.5
57.5	231	5.76	77.2	66.1	73.5
127	232	5.78	77.5	69.5	77.5
801	263	6.27	84.0	73.4	81.4

[a] From eq 4.

Properties of "Monomeric" AM/PSS Complexes. One of the striking differences between the AM/PSS complexes discussed here and the equivalent latex−polyelectrolyte complex is that the apparent molecular weight of the AM/PSS complex is so much higher than the acid micelle itself, by a factor of ca. 20−30 at the lowest AM/PSS mass ratio. In this section we will discuss the limit of low acid micelle concentration because in this case we have the best chance to obtain isolated AM/PSS complex micelles. As we have described in the above, as more acid micelle is added to a fixed amount of PSS, there is a steady increase in the apparent molecular weight and radius of gyration (see Figure 1). We ascribe this to the formation of multicentered complex micelles, formed by bridging. In the limit of zero mass ratio of acid micelle to PSS we expect the formation of "monomeric" complex micelles, e.g., only one acid micelle per particle. We extrapolate the lowest two data points in Figure 1a,b to the zero acid micelle limit, and we have tabulated these values in Table 2. We note that the data for the different molecular weight PSS samples tend to converge in this limit, but a systematic molecular weight effect does persist.

In our previous studies of "onion micelles" formed by cotitration of the acid micelles with PVP-*b*-PEO, we used the following expression for $(MW)_{app}$ as derived from standard static light scattering theory:[6]

$$(MW)_{app} = M_{AM}\left[1 + \frac{c_{PSS;ads}}{c_{AM}}\frac{(dn/dc)_{PSS}}{(dn/dc)_{AM}}\right]^2 + M_{PSS}\left[\frac{c_{PSS} - c_{PSS;ads}}{c_{AM}}(dn/dc)_{PSS}\right]^2 \quad (1)$$

In this equation we have the following definitions: M_{AM} = molecular weight of the acid micelle (13.4×10^6 g/mol); M_{PSS} = molecular weight of the PSS; $(dn/dc)_X$ = the refractive index increment for species X; c_{AM}, c_{PSS} = concentration of the two components; $c_{PSS;ads}$ = concentration of PSS that is adsorbed onto the complex micelle (note: $c_{PSS;ads} + c_{PSS;bulk} = c_{PSS}$).

In our previous work we also used the following definition:

$$c_{PSS;ads}/c_{AM} = \delta \quad (2)$$

For the present experiments M_{PSS} is much smaller than M_{AM}, so we ignore the second term in eq 1. This is also consistent with what we observe experimentally, i.e., under the photodetector gain conditions suitable for light scattering studies of micelles the PSS is undetectable.

We can use eq 1 to obtain δ, and from this we can obtain the corrected molecular weight for the "complex micelle" (cm):

$$(\mathrm{MW})^0_{\mathrm{cm}} = M_{\mathrm{AM}}(1 + \delta^0) \tag{3}$$

where the superscript 0 denotes the zero concentration limit.[14] The values of δ^0 are given in Table 2. The value of δ^0 varies with the molecular weight of the PSS varies systematically, from 5.4 for PSS(5K) to 6.3 for PSS-(801K).

The values of $(R_G)^2_{\mathrm{app}}$ can also be treated by equations which are analogous to eq 1:

$$(R_G)^2_{\mathrm{app}} = w_{\mathrm{inner}} \frac{(\mathrm{d}n/\mathrm{d}c)_{\mathrm{inner}}}{\langle(\mathrm{d}n/\mathrm{d}c)\rangle} (R_G)^2_{\mathrm{inner}} + w_{\mathrm{outer}} \frac{(\mathrm{d}n/\mathrm{d}c)_{\mathrm{outer}}}{\langle(\mathrm{d}n/\mathrm{d}c)\rangle} (R_G)^2_{\mathrm{outer}} \tag{4}$$

This expression is valid only for spherically symmetric particles ("inner" or "outer" refers to the concentric spherically symmetric regions).[15] In this equation w_X is the weight fraction of component X, and $\langle(\mathrm{d}n/\mathrm{d}c)\rangle$ is the average refractive index of the particle. To make any further progress, we have to propose a physical model.

It we take the "inner" sphere to be identical with the AM, with R_g equal to 33.8 nm (i.e., the unperturbed AM), the weight fraction of the "inner" and "outer" portions to be $1/(1 + \delta^0)$ and $\delta^0/(1 + \delta^0)$, respectively, and dn/dc values of 0.27 (appropriate for AM alone) and 0.147 (appropriate for PSS), we obtain the $(R_g)_{\mathrm{outer}}$ $(= \sqrt{(R_G)^2_{\mathrm{outer}}})$ values tabulated in Table 2. As can be seen, $(R_g)_{\mathrm{outer}}$ is only slightly larger than $(R_g)_{\mathrm{app}}$ for this model, which really reflects the fact that the weight fraction of the PSS is so large.

For these particles we have the situation that R_g is larger than $(R_h)_{\mathrm{eff}}$ (see Table 1). This is not the case for the usual core−corona micelle[16] and suggests that the hydrodynamic behavior of these particles is not like an impenetrable sphere.

SEM Imaging. In previous work on charged polymer micelles we have found it useful to deposit the micelles onto oppositely charged surfaces, followed by AFM or SEM characterization.[17] SEM samples were prepared as described in the Experimental Section, and two representative images are presented in Figure 2. In both cases there is a preponderance of fairly uniform spherical micelles, but there are a few larger aggregates which definitely are not dust particles or microcrystals of NaCl. These particles are rather large (≥200 nm), considering this is a dry state. It is expected that sizes derived from SEM will be significantly smaller than for the solution phase because in solution the PSS "corona" should be fully extended. If such large particles are present in solution, they would dominate the QELS signal and size analysis. While the QELS data demonstrated significant polydispersity (see Table 1), unusually large particles were not observed. Note that the difference in micelle surface density in Figure 2a,b is not meaningful because this depends on the details of the sample preparation. There is also no meaningful difference in the micelle size of the samples, as revealed by higher magnification and improved focus.

We saw many samples in which there were smaller or larger numbers of aggregates and except for the centrifugation process described in the next section, we did not find anything systematic about aggregate formation. In particular, a sample such as illustrated in Figure 2b would have the highest probability for formation of bridged structures, yet its SEM images were unremarkable. On the basis of our experience while clarifying these solutions (next section), we propose that aggregates are formed during formation of the SEM sample and are not representative of any species present in the solution.

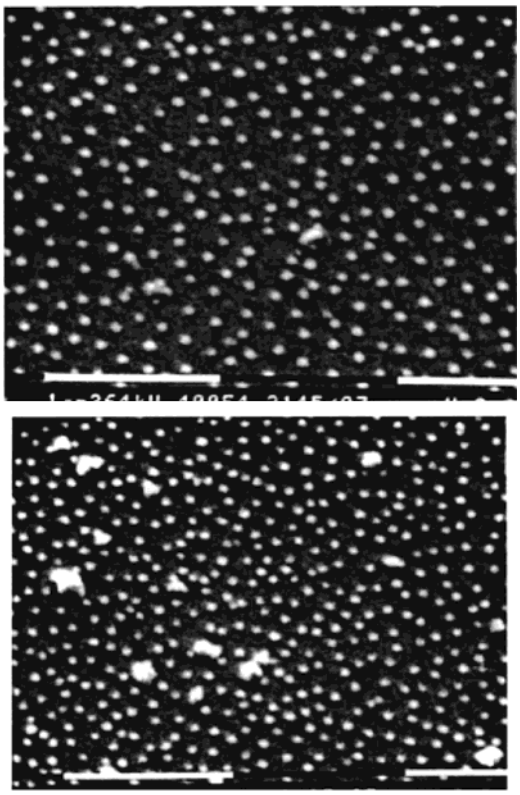

Figure 2. SEM images. In all cases the long white bar is 1000 nm. (a, top) PSS(5K), mass ratio = 0.40; (b, bottom) PSS(801K), ratio 0.25.

Clarification of Samples by Centrifugation and Filtration. Abnormally large molecular weights could be the result of a relatively small mass fraction of large particles. As discussed above, the SEM images often contained some larger particles which could be either aggregates formed during SEM sample preparation or be an intrinsic component of the solution. To try to eliminate such artifacts, we undertook to use two standard solution clarification methods, centrifugation and filtration.

Centrifugation at 5, 10, or 15 krpm for 5 min was carried out (Fisher Scientific Micro 16), and in each case the concentration of the dispersed AM/PSS complex decreased strongly in the upper portion of the solution. There was obvious aggregation of the particles that remained in the supernatant solution, as detected by SEM imaging and QELS. We suggest the following: under the influence of the centrifugal field the massive AM/PSS particles are concentrated near the bottom of the centrifugation tube. At high concentrations the complex particles are unstable and excess PSS is desorbed, leaving behind a significant fraction of nearly neutral complexes, which can aggregate irreversibly. Some of these (10−20%) are redispersed into the upper column of the solution.

Table 3. Characteristics of Filtered Samples

MW (PSS)	c_{AM} (mg/mL)	c_{AM}/c_{PSS}	$MW_{app}/10^6$ (g/mol)	δ	R_g (nm)	$(R_h)_{eff}$ (PD) (nm)
5K	1.19×10^{-2}	0.05	70	2.35	64.1	48.8 (0.25)
	5.95×10^{-2}	0.25	183	4.93	74.7	53.0 (0.15)
	9.52×10^{-2}	0.40	307	6.92	80.0	55.1 (0.17)
57.5K	1.19×10^{-2}	0.05	72.1	2.41	74.7	52.6 (0.13)
	5.95×10^{-2}	0.25	267	6.33	75.2	59.9 (0.14)
	9.52×10^{-2}	0.40	366	7.73	87.7	57.4 (0.14)
801K	1.19×10^{-2}	0.05	150	4.29	77.7	67.9 (0.18)
	5.95×10^{-2}	0.25	424	8.46	87.6	82.2 (0.12)
	9.52×10^{-2}	0.40	807	12.4	113.5	79.8 (0.12)

Table 4. Light Scattering Characterization of Dialyzed AM/PSS(57.5K), $c_{AM} = 8.6 \times 10^{-2}$ mg/mL

NaCl (mM)	$(MW)_{app}/10^6$ g/mol	R_g (nm)	$(R_h)_{eff}$ (PD) (nm)	ζ (mV)
1×10^{-5} [a]	1020	123	80.0 (0.144)	−34.6
1×10^{-2}	912	128	84.0 (0.153)	−31.6
1	964	234	86.2 (0.166)	−34.4
50	203	156	86.5 (0.147)	

[a] PSS background ions in deionized water.

Filtration through 0.45 μm PTFE filters did not induce aggregation although there was significant loss of material (only about 10−20% passed through the filter). The QELS hydrodynamic diameter and apparent molecular weights were reduced by filtration for the three samples studied (see Table 3). The values of δ were still substantial even for the lowest mass ratio of AM to PSS (from 2.4 to 4.3, depending on the molecular weight of the PSS).

We interpret these results as follows: under the modest shear encountered during filtration the PSS chains can be removed from the AM/PSS complex, resulting in significant precipitation inside the filter (the total mass is small so the filter did not become clogged). Those complexes that survived the filtration lost a significant fraction of the bound PSS, yielding lower δ values.

Stability of AM/PSS Complex Micelles at pH 7: ζ-Potenial Measurement. We were interested in obtaining the ζ-potential of the AM/PSS complex, but the ionic conductivity of the pH 1 solution is too high to permit a satisfactory measurement. Therefore, we decided to try to reduce the ionic strength of the solution by dialysis of the AM/PSS(57.5K) complex against pure water or controlled concentrations of NaCl. Naturally the dialysis process simultaneously raises the pH of the bulk solution to 7. It is surprising that the complex is stable at pH 7 because in bulk solution the pyridine groups would be deprotonated, in which case the PSS would be released, and the neutral "acid micelle" would precipitate. We suggest that the favorable ionic interaction between the pyridinium ions and the PSS has made pyridinium a much weaker acid. According to this mechanism, the stability of the AM/PSS complex should depend on the ionic strength. For the lowest ionic strengths (background or 10^{-2} mM) the apparent molecular weight is approximately 1.5 times larger than that of the corresponding solution at pH 1, and the R_g value is essentially the same (cf. Tables 1 and 4). As the ionic strength is increased to 1 mM NaCl, $(MW)_{app}$ decreases but R_g increases significantly. Normally one would expect a polyelectrolyte corona (presumably the PSS) to contract at higher ionic strength.[18] For higher ionic strength the complex micelles aggregate, and even for 50 mM NaCl a precipitate was observed in some cases. We interpret this to be the result of the ionic strength-induced deprotonation of the pyridine groups, with a destabilization mechanism as described above.

We were able to measure the ζ-potential of the three lowest ionic strength dialyzed AM/PSS complex micelles at pH 7. The value of the negative ζ-potential was independent of ionic strength within experimental error (Table 4). The Debye length (κ^{-1}) for the 1×10^{-2} and 1 mM NaCl solutions is approximately 96 and 9.6 nm, respectively. Since the product κR_h is not much smaller than unity, we cannot estimate the charge density of the AM/PSS complex micelles at the shear plane, but we can be sure that there is excess negative charge from the adsorbed PSS.[19]

Discussion

It is reasonable to compare our results to the complexation of polymer latexes with an oppositely charged polyelectrolyte. An example of such a study is the paper by Dautzenberg et al.[5] The anionic latexes studied had a radius of 40 nm with 2.3×10^4 total charges and a molecular weight of 166×10^6 g/mol.[20] The 10 times larger molecular weight of the latex compared to the that of AM of similar size illustrates the much higher overall density of the latex particle. The latex solution was mixed with protonated poly(diallyl dimethylammonium) chloride (MW = 140K). Just as in the present case, the order of addition of the latex and polycation is important. Adding a small amount of polycation to the latex can cause flocculation via bridging. Addition of a larger amount of polycation redisperses the latex up to the point of electroneutrality, at which point aggregation and precipitation occur. Reversing the order of addition by adding latex to concentrated polycation produces stable latexes, just as in the present case, but the increase in the mass or hydrodynamic diameter of the polycation−latex complex is very small, less than 2%, in strong contrast to the results presented herein. It is not stated whether the latex−polycation complex acquires an overall positive charge, but this would be expected on the basis of the conditions of particle formation.

Another study that provides a nice comparison to the present paper is due to Sukhishvili et al.[21] In this case the polycation (poly(*N*-ethyl-4-vinylpyridinium) bromide) was adsorbed onto a carboxylated polystyrene latex particle. The charge density on the polystyrene latex is a strong function of pH, and at pH 11 the maximum ratio of adsorbed cationic groups to surface anion groups is approximately 1.4 (i.e., there is charge overcompensation). These workers also note that the adsorption of the polycation significantly shifts the pK_a of the surface carboxylates.

The result that we wish to emphasize in this paper is the usually large mass and charge overcompensation that we observe. We choose to discuss the results of the extrapolation to zero AM concentration because in this limit the potential for the formation of bridging structures or aggregation of neutral particles during the AM/PSS association is minimized. There is no doubt that large aggregates are formed for the AM/PSS mass ratios outside the range presented in Table 1 or Figure 1, based on the obvious turbidity of the solution, as well as strong changes in the inelastic and static light scattering just below this concentration range. Over the entire concentration range studied there is no QELS evidence for the formation of large extended structures (see $(R_h)_{eff}$ values in Table 1), despite the systematic

increase in $(MW)_{app}$ and R_g. There is no a priori justification for our linear extrapolation to zero AM concentration, and this choice was made pragmatically. The relatively low sensitivity of our QELS apparatus prevented us from going to lower AM concentration to test this dependence.

The mass excess is only weakly dependent on the molecular weight of the PSS.[22] As the degree of polymerization of the PSS goes from ca. 1/10 to ca. 15 times larger than the degree of polymerization of the acid micelle corona polymer, the values of $(MW)^0_{cm}$ and R^0_g change by only about 15−20% (see Table 2). The mass ratio of a PSS monomer to either styrene or 2-vinylpyridine is ca. 1.85. However, the actual physical association of the PSS with the AM must be via the PVP corona, which constitutes 0.62 weight fraction of the micelle. Therefore, the expression

$$\left(\frac{N_{PSS}}{N_{PVP}}\right)^0 = \frac{\delta^0}{(1.85)(0.62)} = 0.87\delta^0 \qquad (5)$$

yields the number ratio of PSS monomer units to PVP monomer units in the complex micelle. Adsorption of PSS may also enhance of the fraction of protonated pyridine groups in the interior of the micelle because the PSS provides a high local ionic strength with relatively small loss of entropy, unlike small counterions (these ideas are illustrated in Scheme 1). If we assume that all pyridines are protonated and each Cl^- counterion is replaced by a styrene group, the mass increase per pyridine unit would be approximately 135 amu, so $\delta \approx (0.62)(135/104) \approx 0.80$ could be rationalized on this basis alone. However, our values of δ^0 are significantly in excess of this value. In fact, if we use eq 5, the ratio of PSS monomer units to PVP monomer units ranges from 4.7 to 5.5. How can this be understood, assuming that it is not the result of some experimental artifact?

The subject of charge overcompensation has been discussed in several recent papers.[23−26] In the first two papers overcharging is discussed for the case that the total charge on a linear polyelectrolyte (PE) exceeds the number of charges on an oppositely charged inflexible macroion that has a much larger cross-sectional area than the PE (a charged cylinder for Park et al.[23] and a sphere for Mateescu et al.[24]). The basic physical concept is that a portion of the linear PE is used to neutralize the surface charge of the macroion, and the remaining "dangling" PE results in a net excess charge. At least in the paper of Mateescu et al. it is stated explicitly that no charge overcompensation is expected if the total charge of the PE does not exceed the total charge of the macroion. Thus, in the context of our experiments one might be able to use these theories to rationalize the values of δ^0 we observe for PSS(801K), but certainly not PS(5K). Gurovitch and Sens propose a Schroedinger-like equation for a charged spherical particle of charge $-Qq$ and a linear polyelectrolyte of charge fNq (f = fraction of charged segments, N = number of segments in the polyelectrolyte) and obtain $fN/Q = 15/6$.[24] While their treatment explicitly considers one chain, it seems likely that multiple chains could be treated similarly. Also in their treatment f is considered to be relatively small, which is not the case for PSS. In a very recent paper by Nguyen et al.,[26] the central role of the correlation between multiply charged ions (including the case of a polyelectrolyte) and the charged object leads naturally to strong charge inversion. None of the specific cases considered in this paper seem to be a good match for the system discussed herein, but for several of the models and parameter ranges charge inversion by factors in excess of five are obtained. Therefore, our results are not difficult to rationalize on the basis of fundamental, if nonintuitive, physical concepts.

Scheme 2

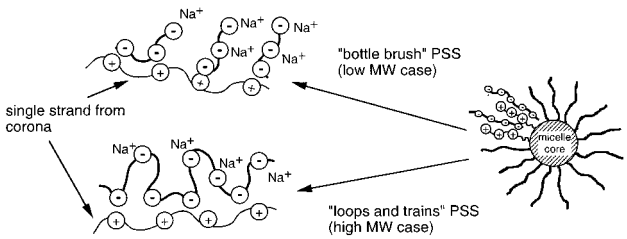

Of course, in our experimental systems the two pendent groups involved are aromatic moieties which might be expected to interact with each other relatively favorably, especially when the solvent is water. These favorable enthalpic factors, in addition to electrostatics, may push the system toward larger mass and charge overcompensation. It also seems plausible to us that the PSS "macro counterion" may create a high ionic strength localized in the corona, which will encourage additional protonation in the corona, thereby pulling the PSS chains toward the core−corona interface.[27] We suggest is that some fraction of the PSS chains are strongly associated with the $PVPH^+$ chains and some are not, forming structures that are analogous to "loops and trains" that are often evoked in discussing polymers adsorbed onto surfaces (see Scheme 2). In the case of the larger PSS chains it is possible that portions of the PSS extend outside the micelle volume, providing additional overcompensation. For short PSS chains one can imagine a "bottle brush" structure that would be essentially equivalent to the "loops and trains" picture (Scheme 2). We note that δ^0 for PSS(801K) is about one unit higher than for PSS(5K) or PSS(16.6K) (see Table 2). The values of R^0_g are approximately twice that of the AM, but the increase in mass is less than 2^3, which suggests that the structure of the complex micelle is less dense than the AM taken as a whole. We note that the starlike morphology of the AM may be important for this phenomenon. Tran et al. recently studied the ability of linear polycations to penetrate grafted PSS brushes on a planar surface (i.e., a planar polyelectrolyte brush) and found less than complete charge compensation (from 0 to 0.4, depending on the molecular weight of the polycation, poly(benzylvinylpyridinium)).[28]

While the AM/PSS complexes are stable to storage for long periods of time after preparation, they do not seem to be stable against centrifugation or filtration. We have ascribed the former instability to the increased concentration that occurs as centrifugation proceeds. If these particles are charge overcompensated, then as they are concentrated it must be thermodynamically favored for the excess PSS to be stripped away, leaving electrically neutral particles that may aggregate. Likewise, fluid flow through the small pores of a filter may strip away excess PSS, resulting in aggregation and precipitation.

It seems likely to us that formation of these massively overcharged particles may be a result of "kinetic trapping". Obviously the driving force for AM/PSS association is very large. As successive PSS molecules diffuse into the $PVPH^+$ corona from the bulk solution, their

predecessors may become crowded toward the micelle interior. In order for the PSS chains to be stretched along the $PVPH^+$ chains, thereby achieving approximate charge balance, the excess PSS chains must be removed. This step could well involve a significant activation energy because there are a number of electrostatic interactions that must be broken simultaneously in order for any group of segments to move an appreciable distance. This kinetic mechanism suggests that the rate of exchange of PSS in bulk solution with dilute AM/PSS complexes will be slow.

Summary

Complex particles have been formed by adding pH 1 solutions of PS-*b*-$PVPH^+$ "acid micelles" (AM) to a pH 1 solution of PSS^-Na^+. As expected, the anionic PSS associates with the cationic micelle corona. According to our analysis of light scattering data, there is a large mass excess of PSS associated with each AM (i.e., factors of 5−6) in the limit of vanishing AM concentration, which disfavors the formation of bridging structures or other aggregation processes. This works out to be approximately 4.7−5.5 PSS monomer units per pyridine. Surprisingly, the effect of the molecular weight of the PSS is minor. We believe that it is the flexible polymer micelle corona that permits this large degree of overcompensation. We present a physical picture of intracorona formation of either loops and trains or grafted chains of the adsorbed PSS onto the $PVPH^+$ that could account for the observations, but this model has not been subjected to any detailed theoretical analysis.

Acknowledgment. Financial support for this research comes from the National Science Foundation (DMR-9973300) and the Robert A. Welch Foundation (F-356) and is gratefully acknowledged. S.E.W. thanks Prof. B. Shklovskii and Prof. M. Cohen Stuart for very helpful discussions.

References and Notes

(1) (a) *Stabilization of Colloidal Dispersions by Polymer Adsorption*; Sato, T., Ruchs, R., Eds.; Dekker: New York, 1980. (b) *Polymer Stabilization of Colloidal Dispersions*; Napper, D. H., Ed.; Academic Press: London, 1981. (c) *Colloid-Polymer Interactions*; Dubin, P. L., Tong, P., Eds.; ACS Symposium Series 532; American Chemical Society: Washington, DC, 1993. *Macromolecular Complexes in Chemistry and Biology*; Dubin, P., Bock, J., Davis, R., Schulz, D. N., Thies, C., Eds.; Springer-Verlag: Berlin, 1993. (e) *Colloid-Polymer Interactions: From Fundamentals to Practice*; Farinato, R. S., Dubin, P. L., Eds.; Wiley-Interscience: New York, 1999.
(2) Decher, G. *Science* **1998**, *277*, 1232.
(3) (a) Takahashi, D.; Kubota, Y.; Kokai, K.; Izumi, T.; Hirata, M.; Kokufuta, E. *Langmuir* **2000**, *16*, 3133. (b) Hallberg, R. K.; Dubin, P. L. *J. Phys. Chem. B* **1998**, *102*, 8629.
(4) (a) Sukhorukov, G. B.; Brumen, M.; Donath, E.; Möhwald, H. *J. Phys. Chem. B* **1999**, *103*, 6434. (b) Donath, E.; Sukhorukov, G. B.; Caruso, F.; Davis, S. A. M.; Möhwald, H. *Angew. Chem., Int. Ed. Engl.* **1998**, *37*, 2202.
(5) Dautzenberg, H.; Hartmann, J.; Rother, G.; Tauer, K.; Goebel, K.-H. Interaction between Polyelectrolytes and Latices with Covalently Bound Ionic Groups. In *Collid-Polymer Interactions (Particulate, Amphilic, and Biological Surfaces)*; Dubin, P. L., Tong, P., Eds.; ACS Symposium Series 532; American Chemical Society: Washington, DC, 1993; pp 138−152.
(6) Talingting, M. R.; Munk, P.; Webber, S. E.; Tuzar, Z. *Macromolecules* **1999**, *32*, 1593.
(7) *Polymer Handbook*, 3rd ed.; Brandrup, J., Immergut, E. H., Eds.; Wiley-Interscience: New York, 1989; pp VII, 409−484.
(8) Kratochvil, P. *Classical Light Scattering from Polymer Solutions*; Elsevier: Amsterdam, 1987.
(9) Huglin, M. B. In *Light Scattering from Polymer Solutions*; Huglin, M. B., Ed.; Academic Press: London, 1972; Chapter 6.
(10) See ref 8, section 2.3.4, pp 84−86.
(11) (a) Hinds, W. C. *Aerosol Technology*; Wiley-Interscience: New York, 1982; Chapter 4. (b) The functional relationship between a mass increment (d*W*) and diameter increment is given by

$$dW = \frac{1}{\ln \sigma_g \sqrt{2\pi}} \exp\left(\frac{\ln d - \ln d_{eff}}{\ln \sigma_g \sqrt{2}}\right)^2 d \ln d$$

(12) Talingting, R. M.; Ma, Y.; Simmons, C.; Webber, S. E. *Langmuir* **2000**, *16*, 862.
(13) We take the molecular weight of the repeating group to be 194 g/mol, which includes the mass of the initially present Na^+ ions.
(14) δ can be calculated for each $(MW)_{app}$ value, but we do not present these data because the possible effect of bridging structures at higher AM concentrations.
(15) See ref 6 for full expression in the case of two linked particles with a center-of-mass displacement of Δ.
(16) For an impenetrable sphere $R_g/R_h = 0.775$.
(17) Karymov, M.; Procházka, K.; Mendenhal, J.; Martin, T. J.; Munk, P.; Webber, S. E. *Langmuir* **1996**, *12*, 4748.
(18) (a) Guenoun, P.; Davis, H. T.; Tirrell, M.; Mays, J. W. *Macromolecules* **1996**, *29*, 3965. (b) van der Maarel, J. R. C.; Groenewegen, W.; Egelhaaf, S. U.; Laap, A. *Langmuir* **2000**, *16*, 7510.
(19) For the lowest ionic strength solution the large value of κ^{-1}permits the use of the limiting relation, $\zeta = q/4\pi\epsilon R_h$ (Heimenz, P. C. *Principles of Colloid and Surface Chemistry*; Marcel Dekker: New York, 1986; p 747, eq 26). Carrying out this calculation we obtain $q = 87e$.
(20) In ref 5 the molecular weight of the latex is not given directly. It is stated that the surface charge density is 1.12×10^{14} e/cm^2, radius 40 nm, and molar mass per charge of 7350. From these values the molecular weight of the latex is calculated to be 165.5×10^6 g/mol. If we assume the density of polystyrene is 1 g/cm^3 and compute the volume, we obtain 161.5×10^6 g/mol. As described in the Experimental Section, each acid micelle has ca. 7.7×10^4 pyridine groups, so if even one-third of them are charged, the acid micelle contains as many charges as the latex.
(21) Sukhishvili, S. A.; Chechik, O. S.; Yaroslavov, A. A. *J. Colloid Interface Sci.* **1996**, *178*, 42.
(22) This is contrast to the recent report by Harada and Kataoka (Harada, A.; Kataoka, K. *Science* **1999**, *283*, 65) in which it was important to match the lengths of oppositely charged diblock polyelectrolytes mixed with a ratio to ensure charge neutrality in order to form well-defined micellar structures. The particle formation process described in this paper differs strongly from ours in that (a) our micelles are already formed before exposure to the PSS and (b) there is a large excess of PSS during the preparation of the complex particle.
(23) Park, S. Y.; Burinsma, R. F.; Gelbart, W. M. *Europhys. Lett.* **1999**, *46*, 454.
(24) Mateescu, E. M.; Jeppesen, C.; Pincus, P. *Europhys. Lett.* **1999**, *46*, 493.
(25) (a) Gurovitch, E.; Sens, P. *Phys. Rev. Lett.* **1999**, *82*, 339 and follow-up commentary. (b) Golestanian, R. *Phys. Rev. Lett.* **1999**, *83*, 2473. (c) Sens, P. *Phys. Rev. Lett.* **1999**, *83*, 2474.
(26) Nguyen, T. T.; Grosberg, A. Yu.; Shklovskii, B. I. *J. Chem. Phys.* **2000**, *113*, 1110.
(27) Preliminary SCF calculations by Chris Simmons demonstrate the strong effect of the MW of the PSS in penetrating the polymer micelle corona.
(28) Tran, Y.; Auroy, P.; Lee, L.-T.; Stamm, M. *Phys. Rev. E* **1999**, *60*, 6984.

MA001366Z